Archive of Applied Mechanics 68 (1998) 158–168 © Springer-Verlag 1998

Critical behaviour of a Timoshenko beam-half plane system under a moving load

A. S. J. Suiker, R. de Borst, C. Esveld

Summary In this contribution, attention is focused on the problem of a moving load on a Timoshenko beam-half plane system. Both the subcritical and the supercritical state will be analysed via a FE-simulation. The character of the response is explained by the analytical derivation and the elaboration of the eigen-value problem that follows from the characteristic wave equations together with the boundary conditions. It will be demonstrated that also transcritical states can occur. The total number of critical states and the values of the corresponding critical velocities are determined by the beam-half plane stiffness properties as well as the contact conditions.

Key words Critical velocities, subcritical and supercritical state, Mach radiation, dispersion, length scale

1 Introduction

Improvements in rail transport capacity are continuously required to maintain a competitive edge against other forms of transportation. The quest for the increasing transport capacity automatically results in the application of higher train speeds. In order to guarantee the safety of the passengers, it is important to adapt the maximum train speed to critical states of the railway structure (or vice versa), which are governed by considerable amplifications of the track response under possible generation of surface waves. Indeed, in France speed limits have been established on certain parts of the TGV-track, since at cruising speed a clearly visible surface wave was noticed in front of the train.

In this contribution, we will consider the influence of the load speed c_l on the critical response of a Timoshenko beam-half plane model via a finite element analysis, in which a strongly accelerating load is applied to the configuration. The Timoshenko beam takes into account the bending and shear deformations of the compound system of rails, sleepers and ballast, and the half plane models the subgrade. The constitutive behaviour of the structure will be considered as elastic, which is justified since the response under an instantaneous load passage is mainly reversible. Although in the past a complete analytical (steady state) solution for the moving load problem has been derived for various beam-elastic support systems (e.g. [2, 4, 5]), the analytical solution is not known for the current system as a result of the more complex system behaviour. Also the fact that the load accelerates, complicates an analytical approach considerably, so that we have to rely on numerical techniques in order to examine the problem. The analytical treatment in this paper will be limited to the derivation of the dispersion relationships, which show that the lowest critical wave speed c_{crit} of a stiff beam-soft half plane system lies between a value somewhat smaller than the Rayleigh wave speed of the half plane and the shear wave speed of the half plane. The exact value depends on the contact conditions and the stiffness difference between the beam and the half plane. When the beam is rigidly connected to the half plane, the total response range can be divided into a *subcritical state* ($c_l < c_{\text{crit}}$) and a *supercritical state* ($c_l > c_{\text{crit}}$). For a soft beam-stiff half plane system, not only the half plane, but also the beam itself influences the resonance behaviour, resulting in two additional critical wave speeds. Under these circumstances, *transcritical states* ($c_{\text{crit},i} < c_l < c_{\text{crit},i+1}$) emerge, where the subscript i denotes the number of the critical state.

Received 24 February 1997; accepted for publication 23 July 1997

A. S. J. Suiker, R. de Borst, C. Esveld
Delft University of Technology, Department of Civil Engineering
P.O. Box 5048, NL-2600 GA Delft The Netherlands

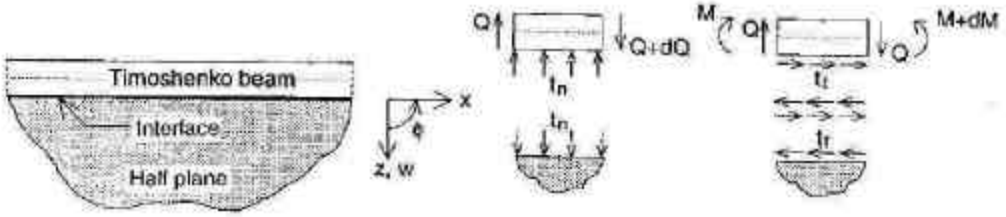

Fig. 1. Timoshenko beam resting on a half plane

Since in practice a stiff beam-soft half plane system is more likely to occur than the opposite situation, a numerical analysis of the former system will be carried out, in which both the subcritical and the supercritical domain are traversed. Because the passage of the critical state yields Mach radiation, this problem shows similarities with the passage of the sound barrier by aeroplanes.

2
Model and governing equations

In Fig. 1 we have depicted the system of a Timoshenko beam that rests on an elastic half plane, where the connection between both elements in the tangential direction is governed by an interface. For a homogeneous half space, the linear relation between the stress tensor σ_{ij} and the strain tensor ϵ_{ij} reads

$$\sigma_{ij} = D_{ijkl}\epsilon_{kl} \ . \tag{1}$$

If we consider the half space as isotropic, the stiffness components D_{ijkl} are expressed by

$$D_{ijkl} = \lambda\delta_{ij}\delta_{kl} + \mu\left(\delta_{ik}\delta_{jl} + \delta_{il}\delta_{jk}\right) \ . \tag{2}$$

Here, λ and μ are Lamé's elastic constants and δ_{ij} is the Kronecker delta. The linearised kinematic relation is given by

$$\epsilon_{ij} = \frac{1}{2}\left(\frac{\partial u_i}{\partial x_j} + \frac{\partial u_j}{\partial x_i}\right) \ , \tag{3}$$

where u_i are the displacements and x_i are spatial coordinates. The equations of motion for the half space read

$$\rho\ddot{u}_i = \frac{\partial\sigma_{ji}}{\partial x_j} + \rho f_i \ , \tag{4}$$

in which ρ is the mass density, $\ddot{u}_i$ are the acceleration components and f_i are the body force components. The equations of motion (4), the kinematic relation (3) and the constitutive relation (1) can conveniently be satisfied by decomposing the displacement vector $\mathbf{u}$ into an irrotational and into a rotational part (see for instance [1])

$$\mathbf{u} = \nabla\Phi + \nabla\times\boldsymbol{\Psi} \ , \tag{5}$$

where $\nabla = (\partial/\partial x, \partial/\partial y, \partial/\partial z)$ and the symbol $\times$ defines the cross product of two vectors. The scalar potential Φ and the vector potential $\boldsymbol{\Psi}$ are the solutions of the three-dimensional wave equations

$$\nabla^2\Phi = \frac{1}{\alpha^2}\ddot{\Phi} \ , \tag{6}$$

$$\nabla^2\boldsymbol{\Psi} = \frac{1}{\beta^2}\ddot{\boldsymbol{\Psi}} \ , \tag{7}$$

in which the compressional body wave (P-wave) speed α reads

$$\alpha = \sqrt{\frac{\lambda + 2\mu}{\rho}} \quad , \tag{8}$$

and the shear body wave (S-wave) speed β is given by

$$\beta = \sqrt{\frac{\mu}{\rho}} \quad . \tag{9}$$

In order to determine the dynamic behaviour for the two-dimensional plane configuration in Fig. 1, the stress components σ_{zz} and σ_{zx} will be expressed in terms of Φ and Ψ by combination of the expressions (5), (3) and (1), leading to

$$\sigma_{zz} = \lambda \nabla^2 \Phi + 2\mu \left(\frac{\partial^2 \Phi}{\partial z^2} + \frac{\partial^2 \Psi_y}{\partial x \partial z} \right) \quad , \tag{10}$$

$$\sigma_{zx} = \mu \left(2 \frac{\partial^2 \Phi}{\partial x \partial z} + \frac{\partial^2 \Psi_y}{\partial x^2} - \frac{\partial^2 \Psi_y}{\partial z^2} \right) \quad . \tag{11}$$

For the current model, the beam cross-section per m width equals $A = 2H \times 1.0\ \mathrm{m}^2$, where $2H$ represents the total beam height. By neglecting higher order terms, the equations of motion for the beam are thus determined by

$$\rho_b A \ddot{w} = \frac{\partial Q}{\partial x} - t_n \quad , \tag{12}$$

and

$$\rho_b I \ddot{\phi} = -Q + \frac{\partial M}{\partial x} + H t_t \quad , \tag{13}$$

where ρ_b is the density of the beam, w is the vertical beam displacement, ϕ is the beam rotation, I is the moment of inertia, Q is the shear force, M is the bending moment, t_n is the interface traction in the direction normal to the beam axis, and t_t is the traction in the direction tangential to the beam axis. The shearing angle of the beam γ is defined by

$$\gamma = \frac{\partial w}{\partial x} + \phi \quad . \tag{14}$$

The constitutive equations with respect to the bending moment M and the shear force Q read

$$M = E_b I \frac{\partial \phi}{\partial x} \quad , \tag{15}$$

and

$$Q = \eta \mu_b A \gamma \quad , \tag{16}$$

in which E_b is the Young's modulus of the beam, μ_b is the shear modulus and η is a numerical factor that takes into account the nonuniform shear distribution with respect to the cross section A.

For the half plane, the boundary conditions at $z = 0$ with respect to the normal stress σ_{zz} and the shear stress σ_{zx} yield

$$\sigma_{zz(z=0)} = -t_n \quad , \tag{17}$$

and

$$\sigma_{zx(z=0)} = +t_t \quad . \tag{18}$$

When the expressions (10) and (11) are substituted in (17) and (18), followed by substitution of (14) to (18) into the equations of motion (12) and (13), we obtain

$$\rho_b A\ddot{w} = \eta\mu_b A\frac{\partial}{\partial x}\left(\frac{\partial w}{\partial x}+\phi\right)+\left[\lambda\nabla^2\Phi+2\mu\left(\frac{\partial^2\Phi}{\partial z^2}+\frac{\partial^2\Psi_y}{\partial x\partial z}\right)\right]_{z=0} , \tag{19}$$

and

$$\rho_b I\ddot{\phi} = -\eta\mu_b A\left(\frac{\partial w}{\partial x}+\phi\right)+E_b I\frac{\partial^2\phi}{\partial x^2}+H\mu\left(2\frac{\partial^2\Phi}{\partial x\partial z}+\frac{\partial^2\Psi_y}{\partial x^2}-\frac{\partial^2\Psi_y}{\partial z^2}\right)_{z=0} . \tag{20}$$

Apart from the boundary conditions (19) and (20), also compatibility of the vertical displacement of the beam and the half plane is required at $z = 0$

$$w = u_{z(z=0)} . \tag{21}$$

For the configuration in Fig. 1, and using (5), this condition can be rewritten as

$$w = \left(\frac{\partial\Phi}{\partial z}+\frac{\partial\Psi_y}{\partial x}\right)_{z=0} . \tag{22}$$

The constitutive relation for the interface shear mode reads

$$t_t = D_{tt}\Delta u_t , \tag{23}$$

where D_{tt} is the shear stiffness of the interface and Δu_t is the relative shear displacement, expressed as

$$\Delta u_t = u_{x(z=0)} - H\phi . \tag{24}$$

Using (5), the horizontal displacement at the half-plane surface reads

$$u_{x(z=0)} = \left(\frac{\partial\Phi}{\partial x}-\frac{\partial\Psi_y}{\partial z}\right)_{z=0} . \tag{25}$$

Taking into account the boundary condition (18), Eq. (11) can be substituted into relation (23). Additionally, expression (24) is combined with (25), and the result is subsequently substituted into (23)

$$\mu\left(2\frac{\partial^2\Phi}{\partial x\partial z}+\frac{\partial^2\Psi_y}{\partial x^2}-\frac{\partial^2\Psi_y}{\partial z^2}\right)_{z=0} = D_{tt}\left[\left(\frac{\partial\Phi}{\partial x}-\frac{\partial\Psi_y}{\partial z}\right)_{z=0}-H\phi\right] . \tag{26}$$

The four equations (19), (20), (22) and (26) contain four unknown variables Φ, Ψ_y, w and ϕ. For a plane harmonic wave type, the following solutions can be formulated

$$\Phi = B_1\exp\left[ik\left(ct-F_p z-x\right)\right] , \tag{27}$$

$$\Psi_y = B_2\exp\left[ik\left(ct-F_s z-x\right)\right] , \tag{28}$$

$$w = C_1\exp\left[ik\left(ct-x\right)\right] , \tag{29}$$

$$\phi = C_2\exp\left[ik\left(ct-x\right)\right] , \tag{30}$$

where B_1 and B_2 are the amplitudes of the body waves in the half plane, C_1 and C_2 are the amplitudes of the body waves in the beam, $i = \sqrt{-1}$, c is the phase velocity, $F_p(F_s)$ takes into account the angle of incidence θ between the plane P-wave (S-wave) and the x-axis, as defined by

$$F_p = \tan\theta_{P-\text{wave}} = \sqrt{\frac{c^2}{\alpha^2} - 1} \ , \tag{31}$$

$$F_s = \tan\theta_{S-\text{wave}} = \sqrt{\frac{c^2}{\beta^2} - 1} \ , \tag{32}$$

and k is the wave number

$$k = \frac{2\pi}{L} = \frac{\omega}{c} \ , \tag{33}$$

in which L is the wave length and ω the angular frequency of the wave. Note, that for the 'Eulerian' type of description '$\exp(ct - x)$', the response during the dynamic process is considered with respect to the dynamic reference parameter 'ct'. Nevertheless, the description could equally well be chosen as 'Lagrangian' with '$\exp(x - ct)$', for which the response is considered with respect to the static reference parameter 'x'.

Substitution of expressions (27) through (30) into (19), (20), (22) and (26) results in an eigen-value problem, which can be written in the matrix-form as

$$\mathbf{A}\mathbf{v} = \mathbf{0} \ , \tag{34}$$

where

$$\mathbf{A} = \begin{pmatrix} -\lambda k^2 - (\lambda + 2\mu)k^2 F_p^2 & -2\mu k^2 F_s & \rho_b c^2 k^2 A - \eta\mu_b k^2 A & -i\eta\mu_b kA \\ -2\mu k^2 F_p & \mu k^2 (F_s^2 - 1) & i\eta\mu_b k \dfrac{A}{H} & \rho_b c^2 k^2 \dfrac{I}{H} - E_b k^2 \dfrac{I}{H} - \eta\mu_b \dfrac{A}{H} \\ ikF_p & ik & 1 & 0 \\ -2\dfrac{\mu}{D_{tt}} k^2 F_p + ik & \dfrac{\mu}{D_{tt}} k^2 (F_s^2 - 1) - ikF_s & 0 & H \end{pmatrix} , \tag{35}$$

and the vector $\mathbf{v}$ contains the wave amplitudes $\mathbf{v}^T = (B_1, B_2, C_1, C_2)$.

The determinant of the 2×2 submatrix in the left upper corner of (35) represents the eigen behaviour of the half space as characterised by the well-known Rayleigh wave. The determinant of the 2×2 submatrix in the right upper corner represents the eigen-behaviour of the Timoshenko beam. The eigen-behaviour of the beam-half plane system can be obtained by solving

$$\det(\mathbf{A}) = 0 \ ,$$

which leads to a fourth-order frequency equation. In the next section, the solutions for this eigen-value problem will be derived numerically for various cases.

3
Wave propagation in the Timoshenko beam-half plane system

In this section, we will analyse the eigen-value problem as given by the relation (34). We will discuss the cases of a relatively soft and of a relatively still Timoshenko beam supported by a half plane. The real solutions of the eigen-value problem represent one or more characteristic eigen-modes, that are governed by the propagation of surface waves along the beam-half plane interface. Because a Timoshenko beam is a one-dimensional element, it is not relevant to attribute the emergence of surface waves to a localised area below the beam axis. However, in order to keep the current analysis consistent with contact descriptions for continua, the surface wave is said to emerge at the beam-half plane interface, which is at a distance H below the beam axis.

The surface waves are activated by body waves which are guided by the Timoshenko beam. The wave guidance results from the fact that the dynamic impedance of the beam differs from the dynamic impedance of the half space. Consequently, the beam is denoted as a *waveguide*. A common feature of a waveguide is the introduction of a 'geometric length scale', which is here characterised by the parameter H. Multiplication of the geometric length scale H with the wave number k yields the characteristic length kH, which quantifies the dynamic interaction between the beam and the half plane. The material and geometry parameters for the compound system are given in Table 1. According to this table, we will vary the beam stiffness E_b and the interface stiffness D_{tt}.

Table 1. Material and geometry parameters

Timoshenko beam	E_b (soft)	10×10^6 [N/m^2] ($\alpha_b = 67$ m/s. $\beta_b = 43$ m/s.)
	E_b (stiff)	1000×10^6 [N/m^2] ($\alpha_b = 667$ m/s. $\beta_b = 430$ m/s.)
	ν_b	0.20 [−]
	ρ_b	2500 [kg/m^3]
	η	1.0 [−]
	$2H$	0.9 [m]
Half plane	E	100×10^6 [N/m^2] ($\alpha = 228$ m/s. $\beta_b = 144$ m/s.)
	ν	0.20 [−]
	ρ	2000 [kg/m^3]
Interface	D_{tt} (smooth)	1.0×10^1 [N/m^3]
	D_{tt} (flexible)	5.0×10^7 [N/m^3]
	D_{tt} (rigid)	1.0×10^{15} [N/m^3]

3.1
Soft Timoshenko beam-stiff half plane system

For the current analysis, we assume the tangential interface stiffness to be relatively small, $D_{tt} = 1.0 \times 10^1$ N/m^3, so that the beam is *smoothly* connected to the half space. The Young's modulus of the beam equals $E_b = 10 \times 10^6$ N/m^2, thus, the beam can be characterised as *soft* in comparison with the half plane, $E = 100 \times 10^6$ N/m^2. Figure 2 shows the dispersion relations that have been obtained by solving (34). Apparently, two wave modes emerge, where mode 1 is coupled to the vertical displacement w of the beam, and mode 2 is coupled to the rotation ϕ of the beam. For each mode, we have plotted the relation between the characteristic length kH and the normalised phase velocity c/β as well as the normalised group velocity c_g/β of the half plane. The group velocity c_g is a physical parameter that governs the velocity of the wave energy propagation. It can be derived (see for instance, [1]) from

$$c_g = \frac{\partial \omega}{\partial k} = \frac{\partial (ck)}{\partial k} = c + k\frac{\partial c}{\partial k} \quad . \tag{36}$$

Both wave modes behave in a strongly dispersive manner ($c \neq c_g$) over a large range of kH. For the long-wave limit ($kH \to 0$), the wave velocity of mode 1 approaches the Rayleigh wave velocity ($c_r = 0.91\,\beta$) of the half plane. For mode 2, the phase and group velocity curves are cut off at the long-wave limit $kH = 0.60$, where $c = c_g = \beta$. Because relatively long waves strongly penetrate the half plane, the long-wave limit of a specific beam mode is fully determined by the half plane properties. Although the group velocity c_g of the mode 2 interface wave approaches the half plane shear wave velocity β, it will always be smaller, which means that no wave energy is transferred into the half plane by shear body waves. In Fig. 2, the wave modes as governed by the emergence of surface waves are restricted by

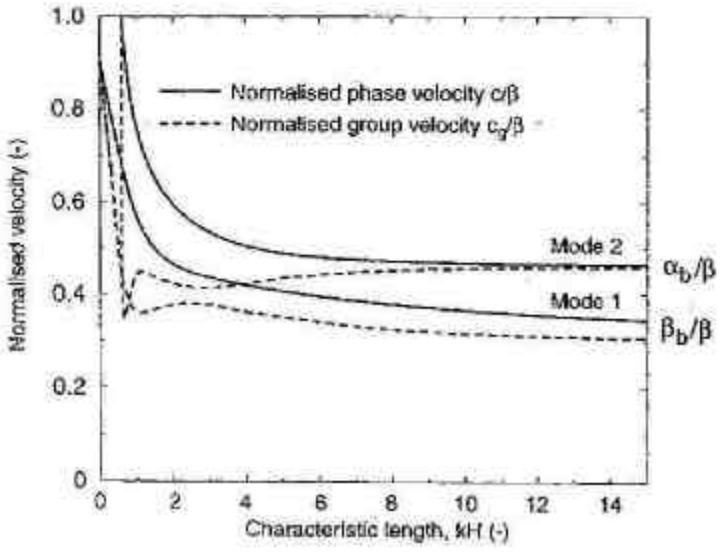

Fig. 2. Dispersion curves for a soft Timoshenko beam-stiff half plane system (smoothly connected, $D_{tt} = 1.0 \times 10^1$ N/m^3)

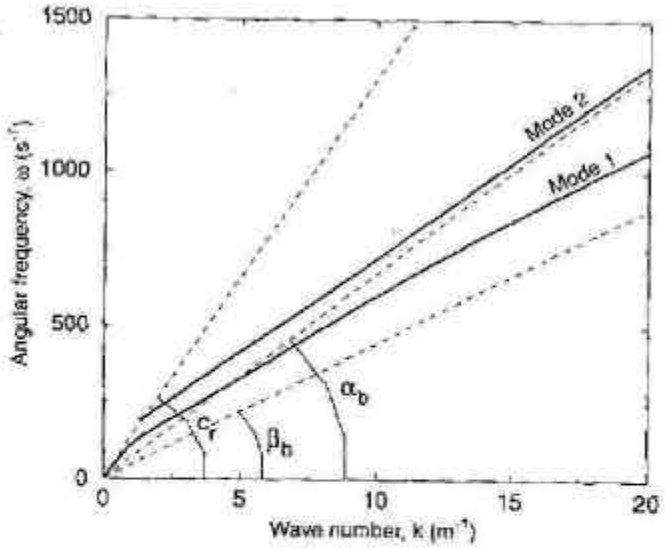

Fig. 3. Dispersion relations in the $\omega - k$ *plane* for a soft Timoshenko beam - stiff half plane system, where $0 < c < \beta < \alpha$ (smoothly connected, $D_{tt} = 1.0 \times 10^1$ N/m^3)

$$0 < c < \beta < \alpha \ . \tag{37}$$

where the determinant of the matrix (35) contains only real terms. This seems logical, since an additional imaginary term would imply that waves are radiated into the half plane (geometrical damping) by body wave transference. Figure 2 reveals also that for the short wave limit ($kH \to \infty$), the wave velocity for the first mode approaches the shear wave velocity of the beam, $\beta_b = \sqrt{\eta\mu_b/\rho}$, while for the second mode it approaches the compressional wave speed of the beam, $\alpha_b = \sqrt{E_b/\rho}$. The character of these limits can be ascribed to the fact that infinite short waves do not penetrate the half plane, so that the corresponding eigen-modes are then fully determined by the beam characteristics.

Although Fig. 2 gives a good impression of the dispersive behaviour of the total system, for moving load problems it is very convenient to plot the dispersion curves in the $\omega - k$ plane, (Fig. 3). By identifying the angular wave frequency ω as a *kinematic invariant* [9], that is expressed as a linear function of the load speed c_l and the load frequency Ω,

$$\omega = \Omega + kc_l \ . \tag{38}$$

the influence of vibrating moving loads with respect to the eigen-behaviour of the system can be plotted in the $\omega - k$ plane by a straight line. When the load frequency Ω equals zero, the kinematic invariant passes the apex. Now, we have three load velocities, $c_l = \beta_b$, $c_l = \alpha_b$ and $c_l = c_r$ at which the kinematic invariant is tangential to the mode 1 and the mode 2 dispersion curves. Since the wave frequency ω and the wave number k are determined by the coordinates of the intersection points of the kinematic invariant and the dispersion curves, the corresponding phase velocity ($c = \omega/k$) of radiated waves as well as the group velocity ($c_g = \partial\omega/\partial k$) will also be equal to β_b, α_b and c_r, as shown in Fig. 3. Hence, for the restriction $c_l = c = c_g$ the energy of radiated waves propagates with the same velocity as the moving load, for which the amount of radiated energy under the load goes towards infinity as time increases. At this state, the load velocity is considered as critical, $c_l = c_{crit}$, and resonance occurs.

3.2
Stiff Timoshenko beam-soft half plane system

Next, the beam stiffness is chosen as $E_b = 1000 \times 10^6$ N/m^2, which is relatively large compared to the half plane stiffness $E = 100 \times 10^6$ N/m^2. We will examine the influence of the interface stiffness, by considering the case of a smooth, $D_{tt} = 1.0 \times 10^1$ N/m^3, a flexible, $D_{tt} = 5.0 \times 10^7$ N/m^3, and a rigid, $D_{tt} = 1.0 \times 10^{15}$ N/m^3, contact condition. For these three cases, Fig. 4 shows the dispersion relations, where, in contrast to the case in the previous section, only one eigen-mode appears. This is due to the fact that the stiffness parameters of the beam are larger than for the half plane, which results in high beam velocities β_b and α_b that will never become critical when the short wave limit ($kH \to \infty$) is approached, as the system prefers to radiate energy into the half plane under *lower* body wave velocities. For this reason, wave modes will not emerge after the characteristic length exceeds a certain value, which limits

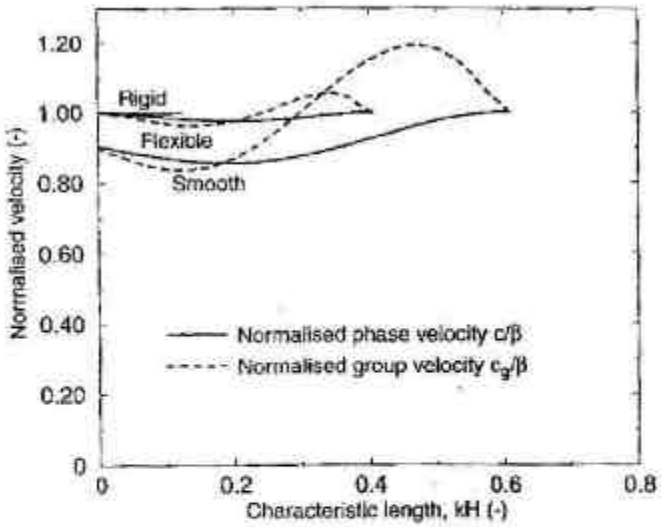

Fig. 4. Mode 1 dispersion curve for a stiff Timoshenko beam-soft half plane system, where $0 < c < \beta < \alpha$; smoothly connected ($D_{tt} = 1.0 \times 10^{1}$ N/m^3), flexibly connected ($D_{tt} = 5.0 \times 10^{7}$ N/m^3) and rigidly connected ($D_{tt} = 1.0 \times 10^{15}$ N/m^3)

the domain kH considerably. For the smooth case, the long-wave limit ($kH \to 0$) approaches the Rayleigh wave velocity of the half plane, while for the flexible case it is slightly *less* than the shear wave velocity, and for the rigid case it almost equals the shear wave velocity. At this stage, the phase velocity c equals the group velocity c_g, so that it can be considered as critical, as explained in Sec. 3.1. However, it appears that the minimum critical velocity occurs at a characteristic length larger than zero. If we consider, for example, the smooth case, at $kH = 0.19$, we have $c = c_g = c_{crit} = 0.85\,\beta$, which is less than the Rayleigh wave velocity at the long-wave limit $c_r = 0.91\,\beta$. At the lowest critical stage, waves travel undeformed through the beam without energy radiation into the half plane ($c < \beta$ and $c_g < \beta$). The occurrence of a critical velocity *lower* than the Rayleigh wave velocity has also been mentioned in [3, 4], where the case is discussed of a continuously moving load on an Euler-Bernoulli beam resting on a half space. Figure 4 clearly reveals that the difference between the lowest critical velocity and the critical velocity at the long-wave limit diminishes when the interface stiffness is increased.

It is also interesting to notice that for the smooth case the phase velocity again equals the Rayleigh wave velocity when $kH = 0.36$. Nevertheless, the corresponding group velocity c_g is now slightly larger than the shear wave velocity β, which causes radiation of wave energy into the half plane. Therefore, at a load velocity equal to the Rayleigh wave velocity the steady state response acts in a critical sense, but it will *not* become infinite since part of the wave energy is dissipated into the half plane so that the resonance is prohibited.

Although we have found two critical velocities for the current set of stiffness parameters, upon further increase of the beam stiffness with respect to the half plane stiffness both critical velocities will tend towards *one* critical resonance velocity, which corresponds to the long-wave limit $kH \to 0$.

For the ranges $0 < \beta < c < \alpha$ and $0 < \beta < \alpha < c$, the frequency equation also contains an imaginary part, implying that waves are radiated into the half plane. Since these ranges do not cover resonance phenomena for reasons explained before, they will be left out of consideration.

4
Numerical simulation

We will now examine the problem of a load that accelerates with $a_l = 100$ m/s^2 from 0 to 180 m/s., on a system of a relatively stiff Timoshenko beam resting on a soft elastic half plane. The connection between the half plane and the Timoshenko beam is modelled as *rigid*. Here, the Timoshenko beam takes into account the bending behaviour of an equivalent ballasted track consisting of rails, sleepers and ballast, while the half plane models a sandy subgrade. In correspondence with the material parameters in Table 1, the half plane body wave velocities are equal to $\beta = 144$ m/s. and $\alpha = 228$ m/s, while the beam body wave velocities are equal to $\beta_b = 430$ m/s. and $\alpha_b = 667$ m/s. In the previous section we have shown that the critical state will be reached when the load speed c_l equals the shear wave velocity β. Hence, the analysis covers the subcritical and the supercritical regime.

The dimensions of the system are $l \times h = 180$ m $\times$ 37.5 m. The half plane is modelled with 1.5 m $\times$ 1.5 m quadrilateral four-noded plane-stress elements, for which a 2 $\times$ 2 Gauss inte-

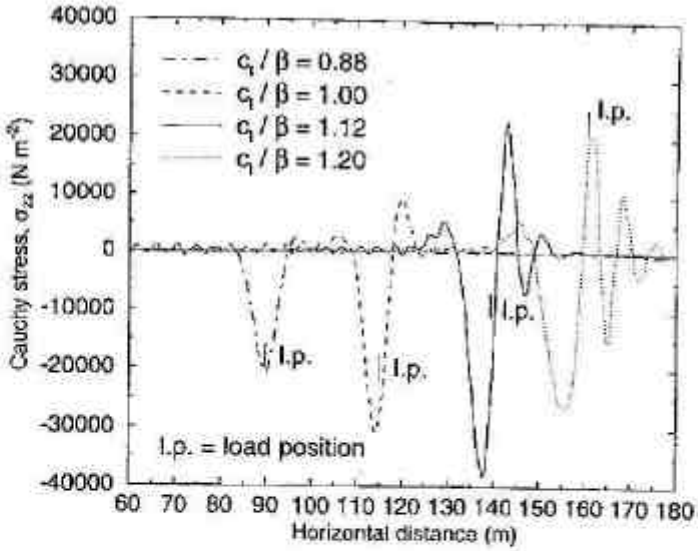

Fig. 5. Vertical Cauchy stress σ_{zz} at 5.68 m below the interface beam-half plane

gration scheme is used. For the beam we have used two-node Timoshenko beam elements with a length $l = 1.5$ m in combination with a two-point Gauss integration scheme. The time integration has been performed using a damped Newmark scheme [6], with the parameters $\beta_{\text{Newmark}} = 0.3025$ and $\gamma_{\text{Newmark}} = 0.6$. The discrete time step equals $\Delta t = 0.002$ s. The mobile character of the load is modelled via a set of discrete pulses that act successively on a sequence of nodes along which the load is suppose to propagate, as discussed in [8]. In order to model the infinite character of a half plane, the wave energy that arrives at the model boundaries needs to be absorbed, since reflections at the boundaries will pollute the physical response. This is done via discrete viscous damping boundary elements, which are orientated perpendicular and parallel to the boundary direction [8].

In Fig. 5 we have depicted the vertical Cauchy stress σ_{zz} at $z = 5.68$ m below the surface, at various load speeds. Obviously, at subcritical load speed, $c_l/\beta = 0.88$, the shape of the response still has a more or less symmetric character. So, despite the fact that the load acceleration is quite large, the appearance of transient waves due to nonstationary load propagation is negligible. When the load traverses the critical velocity $c_l/\beta > 1$, interface waves start to radiate in front of the load position (l.p.). This phenomenon is known as *Mach radiation*. For a load moving with constant velocity (steady state), we have determined in the previous section that the critical response occurs at a load velocity c_l almost equal to the shear wave velocity β. As we can see, the maximum response is generated at a somewhat higher load velocity ($c_l/\beta = 1.12$). This is probably due to the fact that the strong accelerating character of the load ($a_l = 100\,\text{m/s}^2$) causes a small phase shift as a result of the time consumption of radiated body waves. When the acceleration at the critical state would have been negligible, the maximum response probably would have occurred at $c_l = \beta$.

Due to the generation of Mach waves, the response starts to grow in an asymmetrical fashion, where most of the wave energy is radiated in the direction of load propagation. It is furthermore noted that at $c_l/\beta = 1.20$, the response directly below the load acts in an upward sense, which result was qualitatively found also for similar moving load problems [3, 7].

Figure 6 shows stroboscopically the development of the dynamic amplification factor (d.a.f.), which has been obtained by normalisation of the dynamic response (σ_{zz}) with respect to its static counterpart. Initially, the d.a.f. equals 1.0, which corresponds to the static solution. As the load velocity increases, the structure response also increases, where it tends to a maximum of four times the static response when the critical state is reached. Obviously, at this stage, the maximum tensile stress in front of the load position has the same order of magnitude as the maximum compression stress at the load position. After passage of the critical state, the response returns to relatively small amplitudes, comparable to the static value. This kind of behaviour is similar to the passage of the sound barrier by aeroplanes.

Finally, some remarks are made with respect to the magnitude of the dynamic amplification at the critical state. This amplitude partly depends on the load acceleration, while the load acceleration $a_l = 100\,\text{m/s}^2$ considered here has, in fact, an unrealistically high value for a state-of-the-art train vehicle. By choosing a lower load acceleration, the dynamic amplification at resonance will *increase*. At a load acceleration equal to zero (steady state), the resonance

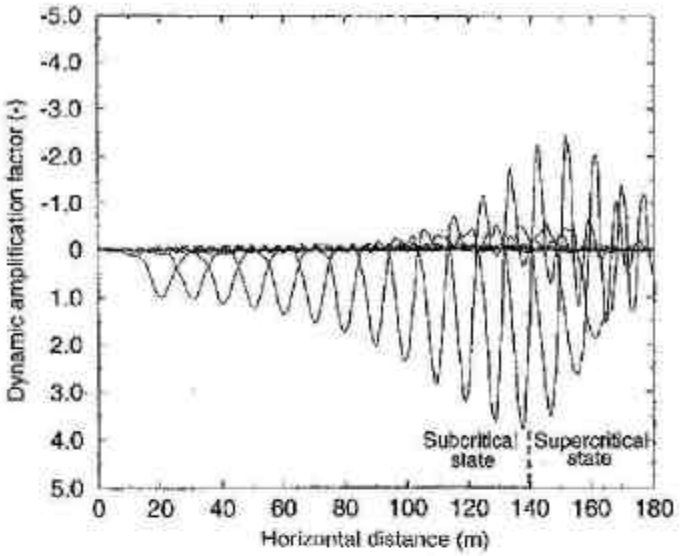

Fig. 6. Stroboscopic development of the d.a.f. as determined by normalisation of a_{zz} with respect to the static solution

response even tends towards infinity. However, the modelling of a realistic load acceleration will lead to extensive consumption of computer time due to the necessity of extremely large elements configurations, which makes it rather unattractive. Furthermore, the dynamic amplification at the resonance state also depends on the amount of structural damping that is caused by physically nonlinear material behaviour, which may *decrease* the dynamic response considerably. For these two reasons, the response amplitude close to the critical state should not straightforwardly be translated into practice.

5
Conclusions and evaluation

It has been demonstrated that a moving load problem can be analysed using the finite element method, in which the moving load is modelled by a sequence of discrete pulses. The response of a Timoshenko beam-half plane model undergoes strong amplifications when a critical state is reached. Generally, a number of critical states can arise, depending on the stiffnesses of the model.

In case of a stiff beam that is smoothly connected to a soft half plane, two critical velocities emerge, where the first critical velocity equals the Rayleigh wave velocity of the half plane, and the second critical velocity occurs at a somewhat smaller value. However, when the interface stiffness or the stiffness difference between the beam and the half plane increase, both critical velocities approach each other, resulting in one critical resonance velocity. Consequently, there is one corresponding resonance state, where passage of this state by a moving load yields a supercritical response, which is strongly asymmetrical as a result of the radiation of Mach waves. When the load speed is further increased, the supercritical response decreases to the order of the static response.

In order to guarantee convenient and safe railway transport, the velocity of a train needs to be considerably smaller (or higher) than a specific critical velocity of the supporting substructure, since the dynamic amplifications around a critical regime may cause unstable vehicle behaviour. Especially when a railway track consists of soft soil bases, such as clay and peat, such problems are likely to emerge since the critical states are then within the velocity domain of a high-speed train.

References

1. **Achenbach, J. D.:** Wave propagation in elastic solids. Amsterdam: Elsevier Science Publishers b.v. 1993
2. **Achenbach, J. D.; Sun, J. T.:** Moving load on a flexibly supported Timoshenko beam. Int. J. Solids Struct. 1 (1965) 353–370
3. **Dieterman, H. A.; Metrikine, A.:** The steady state displacements of a beam on an elastic half space due to a uniformly moving load. Technical Report, Department of Civil Engineering, Delft University of Technology: 1995
4. **Dieterman, H. A.; Metrikine, A.:** The equivalent stiffness of a half-space interacting with a beam. Critical velocities of a moving load along a beam. Eur. J. Mech. A 15 (1996) 67–90
5. **Fryba, L.:** Vibration of solids and structures under moving loads. Groningen: Noordhoff International Publishing 1972

6. **Hughes, T. J. R.:** The Finite Element Method, Linear Static and Dynamic Finite Element Analysis. New Jersey: Prentice-Hall International Inc. 1987
7. **Lansing, D. L.:** The displacements in an elastic half-space due to a moving concentrated normal load. Nasa Technical Report, TR R-238, Langley Research Center, Langley station, Hampton, Va. 1966
8. **Suiker, A. S. J.:** Dynamic behaviour of homogeneous and stratified media under pulses and moving loads. Technical Report, 7-96-119-1, Department of Civil Engineering, Delft University of Technology: 1996
9. **Vesnitsky, A. I.:** Wave effects in elastic systems. In: Wave dynamics of machines, pp. 15–30. Moscow: Nauka 1991